PERFORMANCE-OPTIMIZED MICROSTRIP PATCH ANTENNA FOR WIRELESS CAPSULE ENDOSCOPY

Juily N. Tarade[1], Uday Pandit Khot[2]

[1]Electronics and Telecommunication Engineering Department, Ramrao Adik Institute of Technology, Nerul, Navi Mumbai, Mumbai University, Maharashtra, India

[2]Electronics and Telecommunication Engineering Department, St. Francis Institute of Technology, Borivali, Mumbai University, Maharashtra, India

Abstract: *Compared to standard endoscopy, wireless capsule endoscopy with non-invasive antennas has gained more attention. Since the transmitting antenna of a wireless capsule endoscope (WCE) is located inside the body as opposed to the receiving antenna, which is located outside of it, designing the transmitting antenna is a difficult challenge. Simultaneously achieving high data rates, small size, omni-directionality, acceptable specific absorption rate (SAR), and large bandwidth in telemetry systems are major hurdles faced by these antennas. This is because many parts of the gastrointestinal tract have different dielectric constants and thicknesses. To overcome these obstacles, antennas must be characterized for WCE. With a modified partial ground plane, the suggested antenna is a small planar slotted microstrip patch antenna. It is a miniature ingestion-capable Ultra-Wide Band (UWB) antenna. The substrate material for the antenna is Rogers TMM 13i. An environment that roughly represents the full human gastrointestinal (GI) tract, including surrounding tissues is created using the High Frequency Structure Simulator (HFSS 13.0). The performance of the antenna is evaluated by placing it in the middle of the various GI tracts. The suggested antenna's dimensions are 40 mm3 (10 mm × 10 mm × 0.4 mm) and is a mere 1.26 percent of the capsule's volume. About 4.3 GHz and 6.7 GHz, with a -3 dB bandwidth of about 20.4 MHz and 950 MHz, respectively, are the resonant frequencies. The advantage of having multiple resonant frequencies is that the proposed single antenna can be used for all the GI tract although the dielectric constant varies over the entire GI tract. The existing literature needs different antennas for different GI tracts. In the biological model, the radiation pattern is circularly polarized and omnidirectional. The maximum radiation efficiency of 95.65% has been observed. For the purpose of biocompatibility analysis, the SAR value in the GI tract is also calculated and is in well limit.*

Keywords: **Electromagnetic Bandgap, miniaturization, non-invasive, specific absorption rate, wireless capsule endoscopy**

1. INTRODUCTION

Today's cutting-edge wireless capsule endoscopy technology replaces the conventional endoscopy method, which uses a wired endoscope to diagnose the digestive tract. Due to the fact that endoscopy can only access the duodenum, which is the upper portion of the small intestine, because of its horrible consequences, particularly in younger aged individuals and children [1]. A contemporary non-invasive method for diagnosing life-threatening conditions including inflammatory small intestinal diseases like Crohn's disease is called wireless capsule endoscopy. Cancer, colon polyps, tumours, and gastrointestinal bleeding in the digestive tract that, if discovered at preliminary phases [1]. Therefore, this diagnosing method which has gained attention recently is of the utmost relevance. The antenna, which transfers image data from the sophisticated CMOS image sensor in the capsule to the on-body receiver antennas, is a crucial part of the wireless capsule endoscopy system. The challenge of designing a miniaturised antenna that can fit into a capsule of this size and still leave room for other essential components like LEDs, a CMOS imager, an antenna, a battery, and other electronics arises from the capsule's size restrictions due to the narrow passageways of the digestive system [1]. An antenna with an omnidirectional radiation pattern is necessary due to the capsule's uncontrollably orientated orientation. Another design problem to satisfy high data rate needs for transmitting high-resolution images at fast frame rates is wide bandwidth. Furthermore, the antenna's broad bandwidth lessens the impact of

significant frequency fluctuations on its performance, allowing it to endure the fluctuating conditions of the digestive system [2]. Recent history reports a great deal of research and advancement in this field.

A compact planar slotted microstrip patch antenna with a modified partial ground plane and resonance frequencies of around 4.3 and 6.6 GHz is the proposed antenna in this research. The design of this structure at UWB frequency offers a significant deal of opportunity for increasing bandwidth and utilizing UWB technology's low power and high penetration capabilities, among other benefits. The size of the proposed antenna is 90 mm3 (10 mm × 10 mm × 0.9 mm) which is only 1.26% of the capsule volume. Normally the capsule is of (26x11 mm^2). The radiation pattern is omnidirectional with circular polarization in the biological model. It is observed that the maximum radiation efficiency is 95.65%. The EBG structure is optimized using the Particle Swarm Optimization (PSO) method in order to reduce SAR. There is significant reduction in SAR values at every stage of GI track. SAR values significantly decrease over the whole GI track. The EBG structure causes a little drop in gain (15.65% decrease in antenna gain in the esophagus at 6.7 GHz as compared to the absence of EBG), but this has no effect on the gearbox because the radiated power (2.89 mW) and radiation efficiency (typically ranges between 40% and 70%) are within an acceptable range. The acceptable range of radiated power is 3.1 mW and radiation efficiency (typically ranges between 40% and 70%) for endoscopy application. There is little impact on the fractional BW. The entire simulations are performed in HFSS 13.0. The antenna design, simulation setup, Reduction of SAR using optimized EBG structure, results and conclusions are organized into sections 2, 3, 4, 5 and 6 respectively.

2. Microstrip Patch Antenna for Endoscopy Application

Figure 1(a) and (b) shows the top view and bottom view of the proposed UWB compact planar slotted patch antenna. The antenna is designed on a Rogers TMM 13i substrate because it has a high relative permittivity (ε_r = 12.85, tan δ = 0.0019) with 0.4 mm thickness. Reduction of the effective wavelength of this miniature antenna is made possible by this tan δ. The patch and ground are made of copper. Table 1 summarizes the dimensions of the proposed antenna.

The radiation property is enhanced by using the partial ground plane. In order to increase bandwidth, the upper corners of the ground are deleted. Additionally, notches are added in the upper center of the ground to improve the bandwidth and impedance matching [3].

In the middle of the patch, a plus (+) form slot is added. In order to maximize the resonance frequency and improve bandwidth, a split ring slot is placed around the slot. By increasing the inductance, such slots lower the patch antenna's Q-factor. The bandwidth is increased since the Q-factor and bandwidth have an

Table 1. Dimensions of Proposed Antenna [3]

Parameters	Values (mm)
Substrate	length = 10, Width (*W*)= 10, Thickness = 0.4,
Patch	C1 = 2.5; C2 = 1.5; C3 = 1.3, S1 = 1; S2 = 0.5; Thickness = 0.25
Feed line	Thickness = 0.25, M = 3.2, F1 = 1.8; F2 = 1.8
Ground	Thickness = 0.25, A = 3; B = 1; C = 2.8283

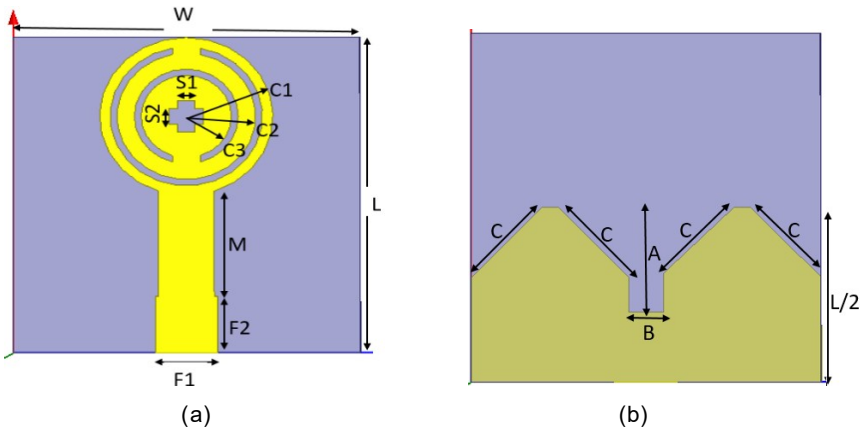

Figure 1. (a) Patch on the substrate (b) Ground under the substrate

inverse relationship. The resonance frequency of these slots is inversely proportional to the patch inductance, which simultaneously reduces the antenna's operational frequency range for a given size. In order to create a single feed, circularly polarized antenna, two square slots were additionally added to the patch's edge [3].

3. Simulation Setup of Proposed Antenna

To study how anatomical factors affect the effectiveness of the transmitting antenna, human models of the stomach, esophagus, small intestine, and large intestine have been built for simulation. The four GI tract models are arranged with the antenna at the center in Figure 2 of paper [4], as discussed in paper [4], and the related simulated results are carried over to the next part. The stomach, large intestine, and small intestine are represented by rectangular boxes, circular cylinders, and spears, respectively, in the same way that the esophagus is represented by a circular cylinder. The four models' tiny dimension values have been chosen for their simplicity of use and speedier processing times.

Size reduction, non-toxic substrate selection, omnidirectional radiation pattern, acceptable SAR preservation, and broad bandwidth maintenance are the fundamental issues facing WCE transmitting antennas. An antenna must be characterized in order to meet each of these requirements. Paper [4] addressed the design, simulation, and analysis of a miniature UWB ingestible capsule antenna for wireless capsule endoscopy. In HFSS, the antenna and its four operational zones, including the gastrointestinal tract, are modelled. According to the modelling results, the antenna has an operating frequency of around 4.3 GHz and 6.7 GHz with a -3 dB fractional bandwidth of about 1.16% and 9.55% respectively. Antenna provides circular polarization with an omnidirectional emission pattern. From comparative analysis it is observed that, the required -3 dB BW of at least 500 MHz for endoscopy application can be achieved at resonant frequency of 6.7 GHz. At 6.7 GHz the peak gain is about 1.6 dBi and the maximum radiated power is 372 mW with radiation efficiency 96.09%. Similarly at 4.3 GHz the peak gain 0.13 dBi, maximum radiated power is 0.430 mW and Radiation efficiency is 6.38%. For better transmission, radiation efficiency need to be improved while antenna travels through small and large intestine. SAR need to be reduce.

Table 2. Comparison of Different SAR Reduction Techniques

Reference	Antenna	Resonant Frequency	Antenna Size	SAR Reduction Technique	Reduction on SAR (%)
[5] 2015	Dipole antenna	900MHz	0.95(ʎ/2) dipole	RF- Shield conductive material (Nickel)	97.7
[6] 2016	PIFA Antenna	1.8 GHz	145x75x10 mm^3	RF- Shield conductive material (Germanium)	92.7
[7] 2017	Circular monopole antenna	2.1GHz 2.45 GHz 3.5 GHz	30x30x0.8 mm^3	Partial SRR	12
[8] 2018	Dipole antenna	0.9 GHz,	(ʎ/2) dipole	Three traditional SRR	84.3
[8] 2018	PIFA antenna	0.9 GHz,	(50×35×0.8) mm^3	One traditional SRR	23.7
[9] 2019	T-shaped planner antenna design	Multiple resonant (2.23, 2.4, 5, 5.8, 3, 3.5, 11.8 and 13.1)	(0.26×0.253×0.0059) λ for frequency 2.23 GHz (35×34×0.8) mm3	Slotted circular shape, and a complementary SRR	13.3
[10] 2020	Mobile phone Model that exists on CST software	BW: (1.62-1.9) GHz, (2.08-2.21) GHz, (4.39-4.99) GHz, and (5.65-6.09) GHz	NA	(4×3) array SRRs and inversed E shaped structure resonator	44
[11] 2021	Rectangular patch antenna, with two SRR	2.5 GHz and 5.5 GHz,	(20×13×1.6) mm^3	Metamaterial slab consists of an (5×3) array of pentagon split ring resonator	84.5
[12] 2021	Mender line patch antenna	2.45 GHz,	(0.1856×0.2088×0.002946) λ	Hybrid SRR	0.651W/Kg
[13] 2021	Mobile phone model that exists on CST software	(1.602, 2.712, and 3.88) GHz	NA	(2×3) hybrid SRR array	upto 36.64
[14] 2019	T-shaped folded dipole antenna	Narrow bandwidth around 2.4GHz	(34×34×0.1) mm^3	Novel design of EBG chip	99
[15] 2020	Oval-shaped monopole antenna	2.45 GHz	(55×59×0.1) mm^3	(3×3) EBG array chip	99.5
[16] 2020	Innovative belt antenna	2.45 GHz,	(31×57×7.6) mm^3	Textile array (4×3) EBG ground plane	98.52
[17] 2021	CWSLMA	2.45 GHz	Antenna:(34×18×1.6) mm3, Antenna with EBG: (78×74×3.6) mm^3	(3×3) array of hexagonal shaped EBG chip	More than 90
[18] 2021	Monopole antenna (2×2) rectangular EBG array with slots	Narrow bandwidth around (2.4, 3.5, and 5.8) GHz	(45.3×34.1×1) mm^3	(2×2) rectangular EBG array with slots	More than 95
[19] 2021	Microstrip antenna	Narrow bandwidth around 26 GHz	(32.1×22×0.35) mm^3	(4×3) EBG array	More than 69.9

4. Reduction of SAR using Optimized EBG Structure

To achieve a low SAR for different antenna applications, a variety of methods are employed. Several other criteria are considered for minimizing the SAR, including directivity, efficiency, gain, bandwidth, and antenna size. However, when taken as a whole, all of these circumstances make it impossible to achieve the intended results. One of the SAR's shortcomings is that it may be unbalanced depending on the technique used to reduce the SAR.

Many strategies are employed to lower SAR, including reflectors, highly directed antenna designs, RF shielding using conductive and ferrite materials, RF shielding using metamaterials like AMC, DGS, SRR, and EBG, and hybrid strategies that integrate two or more strategies simultaneously. Each of these types has unique characteristics that assist determine which application is most appropriate for utilizing them.

4.1. Overview of the SAR

The amount of electromagnetic radiation (EM) that the human body absorbs is referred to as the "specific absorption rate" (SAR). Reaching the worldwide authorized limit for the specified absorption rate (SAR) is one of the most important parts of antenna design. The Institute of Electrical and Electronics Engineers (IEEE) and the International Commission on Non-Ionizing Radiation Protection (ICNIRP) determined the local maximum SAR limits in an uncontrolled environment. The ICNIR Recommendations are the most commonly utilized in Europe. The slightly stricter IEEE standards are used in the US, though. For volume-averaged 10-g data, Australia and Japan have embraced the European SAR restriction of 2 W/kg SAR and for 1-g data it is 1.6 W/kg. Table 3 illustrates the various time durations at which SAR limitations are set [20].

4.2. Metamaterial based on Electromagnetic Bandgap

When constructing antennas for portable communication systems, one of the most crucial aspects to take into account is the Specific Absorption Rate, or SAR. Because the human body can suffer significant harm from the absorption of dangerous electromagnetic waves. Particularly when creating wearable or mobile phone antennas that are in direct contact with the human body. Numerous characteristics, including antenna position, size, and thickness, can be controlled to lower the SAR value. The electromagnetic band gab (EBG) structure is a man-made periodic structure that only helps electromagnetic waves propagate or divert in a due to the periodic variation in the refractive index inside it, a given spectrum of frequencies for all polarization states and all incident angles [21]. EBG gave rise to the method of solving coupled wave equations to gain total control over electromagnetic waves. The dispersion relation revealed that, because of the evanescent waves, there was no wave propagation in a certain frequency band. The EBG structure's composition is comparable to a collection of waveguides and cavities that are frequently employed to regulate the propagation of microwaves [22]. When working with compact antennas, it is better to work with 1-D EBG crystals in order to keep the antenna small, as seen in Figure 2 (a) [23]. The structure of this EBG and its equivalent lumped LC elements is shown in Figure 2 (b) and (c) respectively. Resonant frequency is calculated by equation (1). The inductance and capacitance of the circuit are due to the shorting vias and the spacing between the adjacent metal patches [26] and they are calculated by equation (2) and (3) respectively. However, the Electromagnetic Bandgap (EBG) structure is thought to be among the most significant designs that can be utilized to enhance the antenna performance without sacrificing bandwidth [27]. When compared to the SRR approach, the EBG method is preferable because of the wide range of resonant

and cross polarization effects. As a result, the EBG technique for SAR reduction has gained popularity.

From Table 2, the best approach is to use RF-Shields, particularly when utilizing the EBG substrate. However, when employing one of these techniques to lower SAR value, care must be taken to preserve other crucial elements impacting the antenna's performance, such as impedance matching, which offers high efficiency, shrinks the antenna's size, increases its compactness and robustness, and integrates with the existing RF circuit components.

4.3. Reduction of SAR by Optimizing EBG Structure

The EBG structure is optimized using the Particle Swarm Optimization (PSO) method. A PSO algorithm keeps track of a swarm of particles, each of which stands for a potential resolution. The dispersion analysis is the first step in the design of an EBG structure. The unit cell modelling and application of periodic boundary conditions in the appropriate directions form the foundation of the dispersion analysis. We may determine the precise location of stop bands in the frequency spectrum using the computed dispersion diagram, which is a graphical depiction of the propagation constant's frequency dependency. The PSO algorithm has been tested on a simple planar EBG unit cell depicted in Figure 3 [6].

Table 3. SAR Limits [20]

Region	USA	Europe	Australia	Japan
Organization/ Body	IEEE/ANSI/FCC	ICNIRP	ASA	TTC/MPTC
Measurement method	C95.1	EN50360	ARPANSA	ARIB
Whole body averaged	0.08W/kg	0.08W/kg	0.08W/kg	0.04W/kg
SAR spatial peak SAR	1.6W/kg	2 W/kg	2 W/kg	2 W/kg
SAR averaging time	30 min	6 min	6 min	6 min

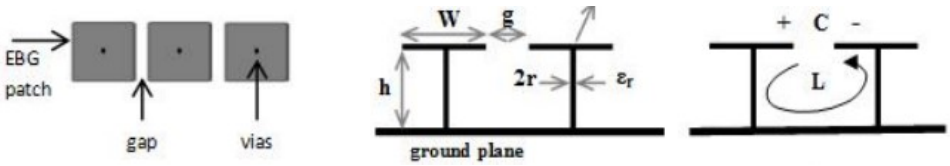

(a) (b)

Figure 2. (a) EBG Patches [24] (b) mushroom like EBG structure [25] (c) Lumpes LC Model [26]

$$f = \frac{1}{2\pi\sqrt{LC}} \tag{1}$$

$$L = \mu_0 \mu_r h \tag{2}$$

$$C = \frac{w\varepsilon_0(\varepsilon_r + 1)}{\pi} \cosh^{-1}\left(\frac{(w+g)}{g}\right) \tag{3}$$

The square patch size P and the period D were chosen as the state variables for the optimization. Height h of the dielectric substrate and relative permittivity r are taken as constants to be equal to 12.85 and 0.4 mm, respectively. The TE surface wave's band gap must have a center frequency of f_c = 4.6 GHz. With regard to both the band gap position and the maximum bandwidth, the fitness (or objective) function F is formulated as a two-criterion function. A minimization of the function is planned. The fitness (or objective) function F is given by equation (4). $f_{\min}$ and $f_{\max}$ is given by equation (5) and (6), respectively.

$$F = \left[\frac{f_{\max} + f_{\min}}{2} - f_C \right] - \left[\frac{f_{\max} - f_{\min}}{f_c} \right] \quad (4)$$

$$\text{Where} \quad f_{\min} = \frac{\omega_0}{2\pi} + \frac{1}{2\pi\eta_0 C} \quad (5)$$

$$\text{And} \quad f_{\max} = \frac{\omega_0}{\pi} - f_{\min} \quad (6)$$

In (4.4), f_{min} is the lower limit and f_{max} is the upper limit of the band gap. This fitness function has been used in PSO for optimizing the EBG structure. In equation (4), the first bracket checks for resonant frequency and second bracket checks about symmetry of BW around resonant frequency.
The population consists of 12 individuals, and parameters of the unit cell D and P are defined in intervals of D € <4.0 mm, 8 mm> and P € <0.50D, 0.95D>, respectively.

4.4. Simulation Results

The proposed antenna with EBG Structure is shown in the Fig. 4 (a) The antenna is placed at the center of the esophagus tissue models of the GI tract, as shown in Fig. 4 (b) and corresponding simulations are carried out to by using HFSS ver. 13.0.

4.4.1 S- Parameter and Bandwidth

The reflection coefficient (|S11|) of the ingestible capsule antenna at the center of the esophagus tissue models of GI tract are exhibited in Fig. 5. It is evident from the figure that the antenna resonates at a frequency of 3.62 GHz, and 4.84 GHz, inside esophagus. The magnitude ($|S_{11}|$) of reflection coefficient of the ingestible antenna is -11.01 dB, and -13.52 dB respectively. -3 dB Fractional bandwidth at resonant frequency 3.62 GHz is 10.66% and at 4.84 GHz, it is 9.73%.

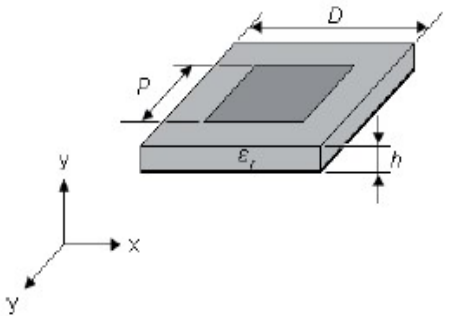

Figure 3. EBG cell under consideration [28]

4.4.2 Radiation Pattern

The 2D far field radiation pattern of the antenna in E-plane and H-plane inside the oesophagus tissue models at the resonant frequencies 3.62 GHz and 4.84 GHz are shown in the Figure 6 (a), (b) and Figure 7 (a), (b) respectively. From the radiation pattern, it is obvious that the antenna exhibits omni-directional radiation pattern throughout the oesophagus. So the antenna will be able to transmit information in all directions independent of the direction and orientation of the capsule which is essential for ingestible antenna.

3-D polar plot inside esophagus tissue model for proposed antenna with EBG is shown in the Figure 8. Maximum gain is about -28 dB at 4.3 GHz and -29.60 dB at 6.6 GHz.

4.4.3 Specific Absorption Rate (SAR)

The simulated distributions of local SAR averaged over 10 g tissue when the capsule antenna with EBG is placed inside esophagus models are shown in the Figure 9 (a) and (b). IEEE C95.1- 2005 standard limits 10g-avg SAR is 2 W/Kg and the IEEE C95.1-1999 standard limits 1g-avg SAR is 1.6 W/Kg. The maximum SAR is calculated for input power of 1W through the esophagus averaged over 10g of tissue is 0.127 W/kg at 4.3 GHz and 1.17 at 6.6 GHz. In order to keep match with IEEE C95.1-2005 standard, the maximum allowable net input power for the proposed design of capsule antenna at 3.62 GHz is 854.3 mW and 736.7 mW at 4.84 GHz. Since Rogers TMM 13i is a ceramic thermoset polymer composite [29], it might be harmless to the GI tract in case of unexpected disruption of the capsule.

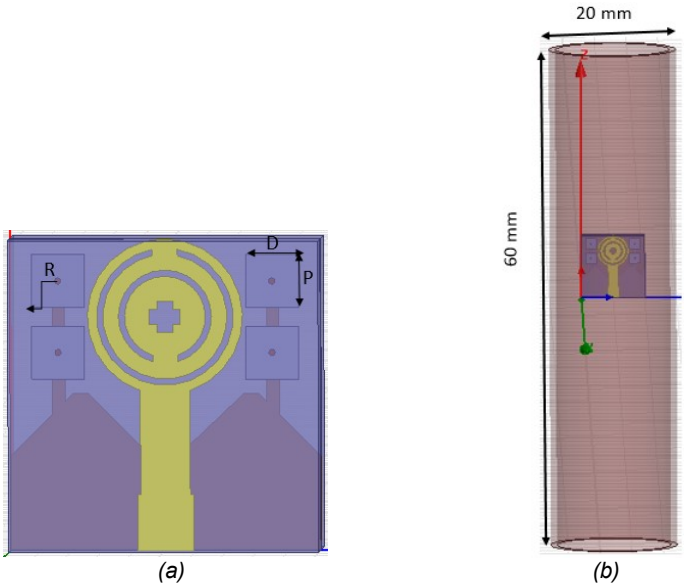

(a) *(b)*

Figure 4. Proposed antenna with (a) EBG Structure (b) antenna with EBG Structure place in Esophagus tissue model

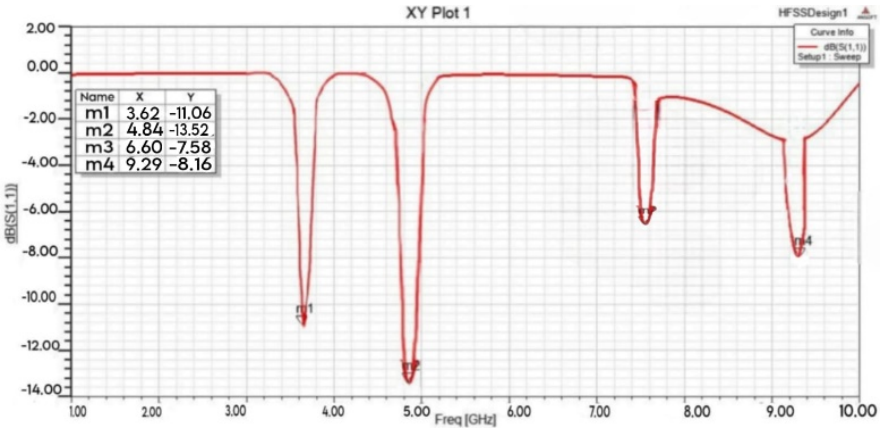

Figure 5. Reflection coefficient frequency responses of the antenna with EBG in esophagus model.

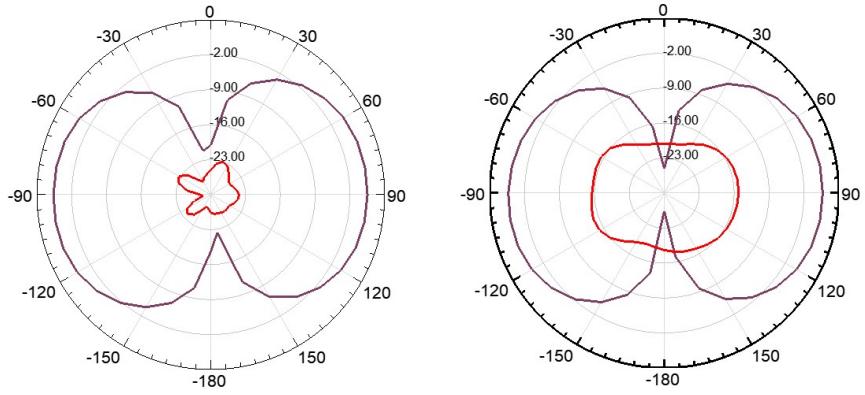

(a) ***(b)***

Figure 6. Far-field directivity radiation pattern of the antenna with EBG at 3.62 GHz through the esophagus tissue model (a) E – Plane (b) H - Plane

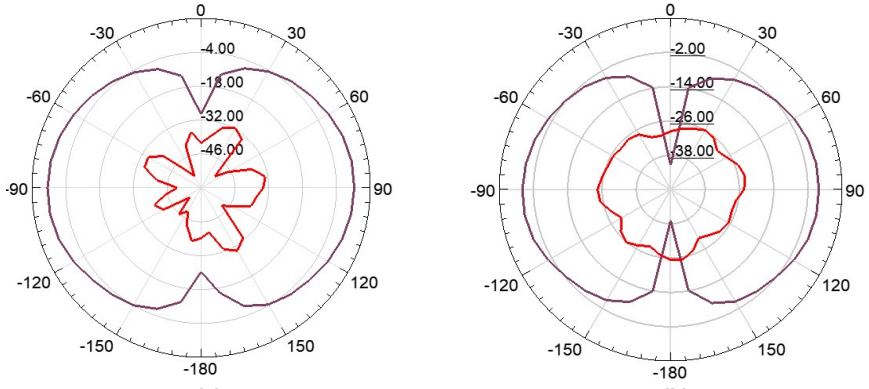

(a) ***(b)***

Figure 7. Far-field directivity radiation pattern of the antenna with EBG at 4.84 GHz through the esophagus tissue model (a) E – Plane (b) H – Plane

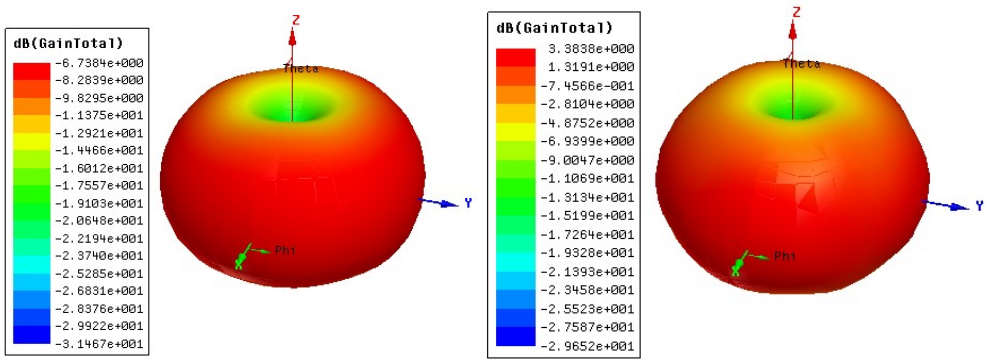

(a) *(b)*

Figure 8. 3-D polar plot of proposed antenna with EBG at (a) 3.62 GHz and (b) 4.84 GHz

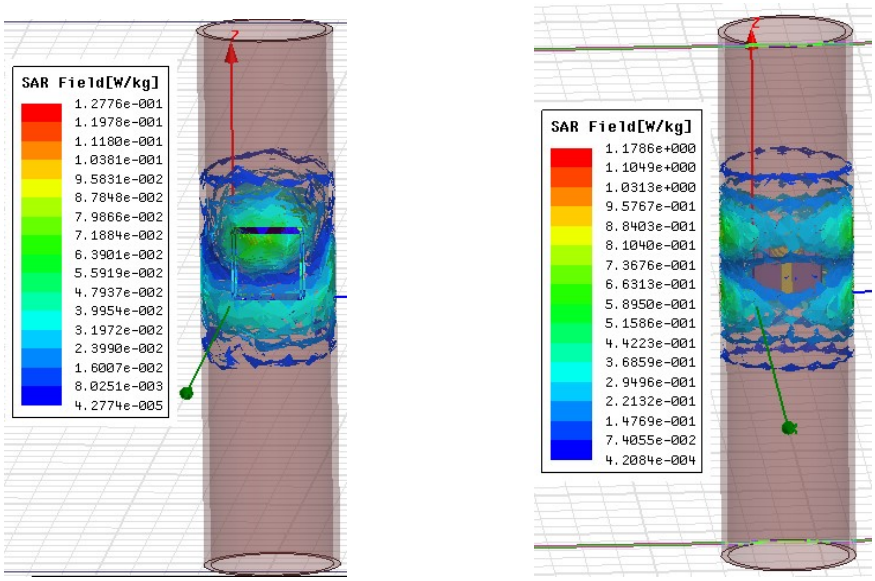

(a) **(b)**

Figure 9. Simulated distributions of local SAR averaged over 1 g tissue for esophagus model at resonant frequency (a) 3.62 GHz (b) 4.84 GHz

5. Comparative Analysis

All performance and safety measures of the ingestible antenna (without EBG) for four different tissue models of GI tract (esophagus, stomach, small intestine, and large intestine for two resonant frequencies are exhibited in Table IV and all the performance measures of the ingestible antenna (with EBG) shown in the Table 5. Table 6 shows Comparison of SAR reduction by using EBG Method. There is significant reduction in SAR values at every stage of GI track. Although because of the EBG structure there is a slight reduction in gain, the radiated power and hence radiation efficiency is in acceptable range which will not affect the transmission. The fractional BW is not getting affected much.

6. Conclusion

Most crucial aspects to take into account is the Specific Absorption Rate (SAR). Because the human body can suffer significant harm from the absorption of

Table 4. Antenna Parameters in Different Tissues at Different frequencies (Without EBG)
(1 Watt i/p Power)

Parameters	Esophagus		Stomach		Small Intestine		Large Intestine	
	4.3 GHz	*6.6 GHz*	*4.3 GHz*	*6.6 GHz*	*4.3 GHz*	*6.6 GHz*	*4.3 GHz*	*6.6 GHz*
|S11|dB	-10.76	-15.34	-9.239	-23.55	-6.102	-4.459	-7.17	-5.077
BW_{3dB} (MHz)	170	760	160	930	140	340	150	390
Fractional BW (%)	3.96	11.51	3.71	14.13	3.24	5.11	3.48	5.90
Radiation Efficiency (dB)	6.38	95.65	5.40	96.09	1.27	35.18	5.10	61.43
Maximum Gain (dB)	-13.75	-18	-12.25	-22.15	16.60	-22.25	-11.70	-11.25
Max. SAR [W/kg]	0.079	40.8	0.0045	7.54	1.368	1050	234	208
Radiated power (Mw)	0.430	276.4	0.372	372.01	$9.48x10^{-5}$	234.05	0.388	79.75
Accepted Power (Mw)	6.738	288.99	6.884	387.12	7.41	665.21	7.60	129.81
Peak Gain(dBi)	0.108	1.6035	0.0688	1.6794	0.0309	0.6130	0.1389	1.1951
Front to back ratio	2.385	1.068	1.2529	1.1004	1.4126	1.7683	2.3193	1.4425
Peak Directivity	1.702	1.6764	1.274	1.7476	2.4188	1.7425	2.7225	1.9452

Table 5. Antenna Parameters in Different Tissues at Different Frequencies (With EBG)
(1Watt I/p Power)

Parameters	Esophagus		Stomach		Small Intestine		Large Intestine	
f_r (GHz)	**3.62**	**4.84**	**3.62**	**4.84**	**3.62**	**4.84**	**3.62**	**4.84**
|S11|dB	-3	-3.1	-10	-11.06	-8.06	-8.09	-8.5	-7.01
BW_{3dB} (MHz)	700	420	370	360	360	340	370	410
Fractional BW (%)	10.66	9.37	9.67	8.12	7.89	9.89	7.23	8.23
Radiation Efficiency (%)	12.3	93.12	2.40	26	2.38	26	12.15	22.95
Maximum Gain (dB)	-28	-29.60	-26.75	-30.30	26.70	-30.30	-27.75	30.25
Max. SAR [W/kg]	0.127	1.78	0.0045	7.45	1.368	2.45	1.06	57..22
Radiated power (mW)	1.798	24.52	0.325	2.89	0.324	2.89	1.76	2.78
Accepted Power (mW)	14.56	26.33	13.5	11.14	13.7	11.14	14.5	12.14
Peak Gain(dBi)	0.211	2.18	0.042	0.68	0.043	0.68	0.20	0.61
Front to back ratio	1.065	1.03	2.56	1.11	2.55	1.11	1.13	1.15
Peak Directivity	1.72	2.34	1.77	2.62	1.81	2.62	1.69	2.66

dangerous electromagnetic waves. Particularly when creating wearable or mobile phone antennas that are in direct contact with the human body. Numerous characteristics, including antenna position, size, and thickness, can be controlled to lower the SAR value. The best approach is to use the EBG substrate. However, when employing this technique to lower SAR value, care must be taken to preserve other crucial elements impacting the antenna's performance, such as impedance matching, which offers high efficiency, shrinks the antenna's size, increases its compactness and robustness, and integrates with the existing RF circuit components. The suggested antenna's dimensions are 40 mm^3 (10 mm × 10 mm × 0.4 mm) and is a mere 1.26 percent of the capsule's volume. About 4.3 GHz and 6.7 GHz, with a -3 dB bandwidth of about 20.4 MHz and 950 MHz, respectively, are the resonant frequencies. The advantage of having multiple resonant frequencies is that the proposed single antenna can be used for all the GI tract although the dielectric constant varies over the entire GI tract. The existing literature needs different antennas for different GI tracts. In the biological model, the radiation pattern is circularly polarized and omnidirectional. The maximum radiation efficiency of 95.65% has been observed. For the purpose of biocompatibility analysis, the SAR value in the GI tract is also calculated and is in well limit. PSO helps in optimizing the dimensions of EBG structure to reduce the SAR. SAR values significantly decrease at each stage of the GI track, as seen in Table VI. While the EBG structure results in a minor decrease in gain, the gearbox will remain unaffected because the radiated power and, thus, radiation efficiency, are within an acceptable range. There is little impact on the fractional BW.

REFERENCES

[1] *R. Mulugu, and C. Saha, "Design, Development and Realization of UWB Antenna for Wireless Capsule Endoscopy," In IEEE Int.Symp. on Antennas & Propag. (APSYM),**2020** December19-21.*

[2] *M. Sarestoniemi et al., "WBAN channel characteristics between capsule endoscope and receiving directive UWB on-body antennas," IEEE access, vol. 8,**2020** March 55953-55968.*

[3] *J. Wang et al., "An Implantable and Conformal Antenna for Wireless Capsule Endoscopy" IEEE Antennas and Wireless Propag. Lett., vol. 17, no. 7, **2018** May 1154-115,.*

[4] *J. Tarade and U. P. Khot, "Characterization of Microstrip Patch Antenna for Endoscopy Application" Int. J. of Electronics and Communication Engineering (IJECE), vol. 11, no. 8, **(2024)**, pp. 207-217.*

[5] *R. B. Rani and S. Pandey, "Mobile phone radiation reduction using shield made of different materials," in 13th Int. Conf. on Electromagnetic Interference and Compatibility (INCEMIC), **2015**, pp. 176-178.*

[6] *P. K. Dutta, P. V. Y. Jayasree, and V. S. S. N. S. Baba, "SAR reduction in the modelled human head for the mobile phone using different material shields," Human-centric Computing and Information Sciences, vol. 6, pp. 1-22, **2016**.*

[7] *S. I. Rosaline and S. Raghavan, "Split ring loaded broadband monopole with SAR reduction," Microwave and Optical Technology Letters, vol. 58, **2016** February 158-162.*

[8] *H. Messaoudi and T. Aguili, "Use of a Split Ring Resonators with Dipole and PIFA Antenna to Reduce the SAR in a Spherical Multilayered Head Model," in 2018 6th Int. Conf. on Multimedia Computing and Systems (ICMCS), **2018,** pp. 1-6.*

[9] R. K. Saraswat and M. Kumar, "A metamaterial hepta-band antenna for wireless applications with specific absorption rate reduction," Int. J. of RF and Microwave Computer-Aided Engineering, vol. 29, p. e21824, **2019**.

[10] A. M. Tamim, M. R. I. Faruque, E. Ahamed, and M. T. Islam, "Electromagnetic absorption of SRR based double-inverse E Shaped metamaterial for DCS, EESC, 5G, and WiMAX applications," Chinese Journal of Physics, vol. 66, **(2020),** pp. 349- 361.

[11] I. Rosaline, "A Triple-Band Antenna with a Metamaterial Slab for Gain Enhancement and Specific Absorption Rate (SAR) Reduction," Progress In Electromagnetics Research C, vol. 109, **(2021),** pp. 275-287.

[12] N. Ganeshwaran, J. Kailairajan Jeyaprakash, and G. N. A. Mohammed, "Compact coplanar waveguide fed implantable antenna with hybrid split-ring resonators," Int. J. of RF and Microwave Computer-Aided Engineering, vol. 31, pp. e22625, **2021**.

[13] T. Ramachandran, M. R. I. Faruque, and M. T. Islam, "Dielectric passive left-handed symmetric metamaterial design for electromagnetic absorption reduction application," Proceedings of the Institution of Mechanical Engineers, Part L: Journal of Materials: Design and Applications, vol. 236, no. 11, **(2021),** pp. 2157-2170..

[14] S. A. Balakrishnan and E. F. Sundarsingh, "Conformal self- balanced EBG integrated printed folded dipole antenna for wireless body area networks," IET Microwaves, Antennas & Propagation, vol. 13, **(2019)**, pp. 2480-2485..

[15] M. E. Atrash, O. F. Abdalgalil, I. S. Mahmoud, M. A. Abdalla, and S. R. Zahran, "Wearable high gain low SAR antenna loaded with backed all-textile EBG for WBAN applications," IET Microwaves, Antennas & Propagation, vol. 14, **(2020),** pp. 791- 799, 2020.

[16] R. Pei, M. P. Leach, E. G. Lim, Z. Wang, C. Song, J. Wang, et al., "Wearable EBG-backed belt antenna for smart on-body applications," IEEE Trans. on Industrial Informatics, vol. 16, (**2020**), pp. 7177-7189, 2020.

[17] S. Singh and S. Verma, "SAR reduction and gain enhancement of compact wideband stub loaded monopole antenna backed with electromagnetic band gap array," Int. J. of RF and Microwave Computer-Aided Engineering, pp. e22813, **2021**.

[18] W. El May, I. Sfar, J. M. Ribero, and L. Osman, "Design of Low-Profile and Safe Low SAR Tri-Band Textile EBG-Based Antenna for IoT Applications," Progress In Electromagnetics Research Letters, vol. 98,**(2021)**, pp. 85-94..

[19] E. Wissem, I. Sfar, L. Osman, and J. Ribero, "A Textile EBG Based Antenna for Future 5G-IoT Millimeter-Wave Applications," Electronics, vol 10, no. 2, **(2021)**, pp. 154-160.

[20] S. I. Al-Mously, "Factors influencing the EM interaction between mobile phone antennas and human head," In Int. Conf. on Digital Information and Communication Technology and Its Applications, (**2011**), pp. 106-120.

[21] P. P. Bhavarthe, S. S. Rathod, and K. Reddy, "A compact dual band gap electromagnetic band gap structure," IEEE Trans. on Antennas and Propagation, vol. 67, **2018** March 596- 600.

[22] M. El Atrash, M. A. Abdalla, and H. M. Elhennawy, "A compact flexible textile artificial magnetic conductor-based wearable monopole antenna for low specific absorption rate wrist applications," Int. J. of Microwave and Wireless Technologies, vol. 13, **(2021),** pp. 119-125.

[23] A. Hediya, A. M. Attiya, and W. S. El-Deeb, "Reduction of specific absorption rate: A review article. The Egyptian International Journal of Engineering Sciences and Technology," vol. 39, no. 3, **(2022),** pp.80-96.

[24] *D. Kurup, W. Joseph, G. Vermeeren, and L. Martens, "Specific absorption rate and path loss in specific body location in heterogeneous human model," IET Microwaves, Antennas & Propag., vol. 7, no. 1,* ***(2013),*** *pp. 35-43.*

[25] *S. Alamri, "Implanted antennas for Biomedical applications," Thesis, University of Sheffield,* ***2016****.*

[26] *M.Fallah and L.Shafai, "Enhanced Performance of a Microstrip Patch Antenna using a High Impedance EBG Structure", Antennas and Propagation Society International Symposium, vol. 3,* ***2003****.*

[27] *N. Melouki, A. Hocini, and T. A. Denidni, "Performance enhancement of a compact patch antenna using an optimized EBG structure," Chinese Journal of Physics, vol. 69,* ***(2021),*** *pp. 219- 229.*

[28] *J. Kennedy, and R. Eberhart, "Particle swarm optimization," In Proc. of ICNN'95- IEEE int. conference on neural networks, vol. 4, pp. 1942-1948, Nov. 1995.*

[29] *Rogerscorp.com, 'TMM® 13i Laminates', 2018 [online]. Available: https://www.rogerscorp.com/acs/products/51/TMM-13iLaminates.aspx. [Accessed: 10- Jan- 2018].*